Computational Fluid Dynamics Study on the Ventilation Flow Paths in Longwall Gobs

Liming Yuan, Alex C. Smith and Jürgen F. Brune
Pittsburgh Research Laboratory
National Institute for Occupational Safety and Health

ABSTRACT: To provide insights and assistances for the optimization of ventilation systems for U. S. underground coal mines facing both methane control and spontaneous combustion issues, a computational fluid dynamics (CFD) study is being conducted to investigate the effect of the ventilation scheme on the prevention of spontaneous combustion in longwall gob areas. This report focuses on the flow patterns within the gob under three different ventilation systems; one-entry and two-entry bleederless systems as well as a three-entry bleeder system. The gas flow in the caved gob area is simulated as a laminar flow through porous media while the gas flow in ventilation airways is simulated as a fully developed turbulent flow. The air flow patterns are visualized using flow path lines. Air velocity contours and vector data are also obtained. The possible location of critical velocity zones where the gob is most liable to spontaneous heating is discussed.

1 INTRODUCTION

Spontaneous combustion continues to be a significant risk for underground coal mines, particularly in U.S. western mines where the coal is generally of lower rank. This hazard is exacerbated in mines with appreciable levels of methane, due to the potential of an explosion ignited by a spontaneous combustion fire. The most recent reported data on mine fires in the U.S. for the period 1990 – 1999 show that there were 15 reported fires caused by spontaneous combustion in underground coal mines, accounting for 17% of the 87 total reported fires (DeRosa, 2004). Although the number of fires is relatively low, amounting to an average of 1 to 2 fires per year, the potential for catastrophic consequences is very high. In fact, three of the mine fires from the reported 1990 – 1999 period resulted in subsequent methane explosions. In addition, although the number of spontaneous combustion fires has remained nearly constant for the last 35 years, there is the possibility that the number of spontaneous combustion fires increases due to growth in the dimensions of longwall panels and due to the exhausting of easily-mined coal beds in the U.S., which results in increased mining of lower rank coals and deeper coal beds.

Most spontaneous combustion fires have occurred in the gob areas of U.S. coal mines. Gob areas, by the very nature, present accessibility problems regarding detection, fairly precise locating, and fire extinguishment. The self-heating of coal occurs when the heat produced by low-temperature oxidation is not adequately dissipated, resulting in a net temperature increase in the coal mass. Under conditions that favor a high heating rate, a fire ensues. The oxidation of coal requires a fuel, the coal, and an oxidizer, usually the ventilation air. To reduce the amount of oxidation, and thus the amount of heat being produced, either the coal or the air must be removed. On the other hand, if the airflow is sufficiently high, it can remove the heat produced by the coal oxidation, and thus prevent acceleration of coal self-heating that may result in a fire. The amount of coal in a retreat longwall gob can be somewhat controlled by the mining practices, such as pillar design and the amount of coal left in the roof and floor. Additional coal from un-mined coal bands immediately above or below the mined seam may be present in the gob as well.

The amount of airflow through a longwall gob can be reduced by using a bleederless ventilation design. In the U.S., bleederless systems are only per-

mitted as a spontaneous combustion control method in mines with a demonstrated history of spontaneous combustion. However, in U.S. mines with appreciable methane levels, ventilating gob areas with bleeder systems to dilute and remove methane has been traditionally regarded as the preferred method to deal with the methane hazard. Bleeder system design can exacerbate the spontaneous combustion hazard in mines with both methane and spontaneous combustion issues.

In order to optimize the airflow in the gob to prevent spontaneous combustion and control the methane content, it is important to understand likely air flow patterns inside the gob and their effect on both coal self-heating and methane migration. Because much of the gob area is inaccessible, it is difficult to measure the air flow rate in it. Although some field measurement methods such as tracer gas technology have been used to determine the air flow pattern, the results are limited. Therefore, flows through the caved area of the gob and even to some extent along the periphery have been mainly conjecture based on spotty experiences or investigations. Absent practical methods to gather empirical data, controlled modeling techniques are viewed as the only current reasonable way to assess the ventilation in gob areas.

Computational Fluid Dynamics (CFD) modeling has been increasingly applied to mine ventilation in recent years. CFD is the application of numerical techniques to solve the Navier-Stokes equations for fluid flow. The Navier-Stokes equations are derived by applying the principles of conservation of mass and momentum to a control volume of fluid and are solved by discretizing the equations using either finite difference or finite element techniques. In Australia, Balusu et al. (2002) and Wendt & Balusu (2002) conducted CFD modeling of longwall gob air flow dynamics with focus on bleederless ventilation systems. In the U.K., Ren et al. (1997) performed CFD modeling of methane flow around longwall coal faces. All these studies were based on specific ventilation schemes, and results were limited to those ventilation systems. In the U.S., Wala et al. (2003) have used CFD to evaluate aspects of mine face ventilation, but no CFD work has been done to model flows in the longwall mine gob area. Brune et al. (2000) identified the significant changes for U.S. longwall mine ventilation and studied the effects of different bleeder configurations and ventilation adjustments. Longwall gob leakage was also simulated using a ventilation network analysis program, VNET, by Brunner (1985) and Banik et al. (1995).

NIOSH has initiated a new program to develop CFD models to evaluate ventilation schemes to control spontaneous combustion and to describe the ventilation pathways through the immediate gob and to evaluate their effect on gob methane control systems. In this paper, a preliminary CFD study of air flow patterns in the gob is presented.

2 VENTILATION SCHEMES

The increase of longwall panel lengths and widths in the U.S. continues to present challenges to longwall mine ventilation systems. Among these challenges is the characterization of flow patterns through and around the gob, and the effect of these airflows on the spontaneous combustion risk.

Three types of ventilation schemes were investigated to demonstrate the air flow patterns in the gob. The simulated gob area in the three studies is 1000 m long, 300 m wide and 50 m high starting from the bottom of the coal seam, representing a typical longwall panel layout in the U.S. The caved region may have a height of 3 ~ 4 times mining height, but a highly fractured region may extend beyond that height. The 50 m height was chosen to cover both the caving and highly fractured regions. Although actual longwall panel lengths extend to 3,000 or 4,000 m, a 1,000 m section was selected to model the flow paths in this study. The ventilation airway dimensions are 2 m high by 6 m wide, and the longwall face is 4 m wide by 2 m high.

The first ventilation scheme is a simple "U" bleederless ventilation system with one entry, as shown in Figure 1 (a). The second scheme is a two-entry bleederless system as shown in Figure 1 (b). For the convenience of simulation, two intake entries were combined into one entry, and only one crosscut close to the face was open to the second return entry. The third ventilation system, shown in Figure 1 (c), is a three-entry bleeder system. The three collapsed entries at the tailgate side were combined into the gob area and were connected to the bleeder fan through an open entry. It should be pointed out that this treatment may be only valid near the end of the panel life. During the earlier stages of the panel life, the middle entry remains at least partially open and has a different airflow resistance than the collapsed area. It then serves as a primary route for bleeder air. With the retreat of the longwall face, the middle entry continues to collapse, and will have a same order of magnitude resistance as other collapsed areas approaching the end of the panel life. On the headgate side, the belt entry was combined with the intake entry and the flow rate in both entries was taken into account. All crosscuts between the second and third entries on the headgate side were open. Although intact stoppings may be maintained between the second and third entry for

some longwalls for the purpose of methane dilution, it will not affect this model significantly. The bleeder entries at the back end of the gob were also combined into one model entry connecting to the bleeder fan.
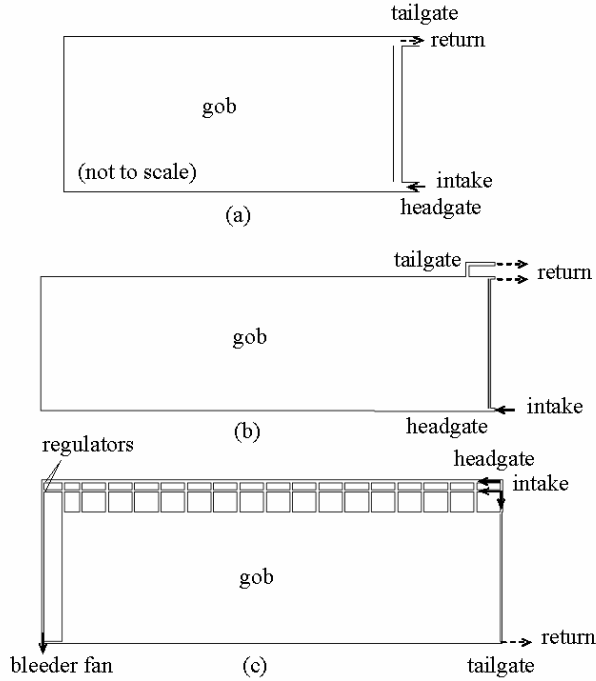

Figure 1. Ventilation schemes: (a) one-entry bleederless system; (b) two-entry bleederless system; (c) three-entry bleeder system.

3 ESTIMATION OF GOB PERMEABILITY

It is generally believed that the permeability inside a gob varies in different areas. The global permeability distribution within the gob of a single longwall panel was represented by five constant-permeability zones, as shown in Figure 2. The division of the gob area and the assignment of permeability data were based on geotechnical modeling of longwall mining and the associated stress-strain changes/rock failure using FLAC (Fast Lagrangian Analysis of Continua) code (Esterhuizen & Karacan, 2005). In FLAC modeling, mining was simulated in increments, starting from one side of the grid and advancing to the other side. Extraction of the coalbed was modeled by removing elements over the height of the coalbed. The process of gob formation was modeled by first deleting rock elements in the roof of the coalbed, so that they are stress relieved, followed by inserting gob properties in these elements. Gob properties were also inserted in previously mined coalbed elements, so that the gob filled the mined void.
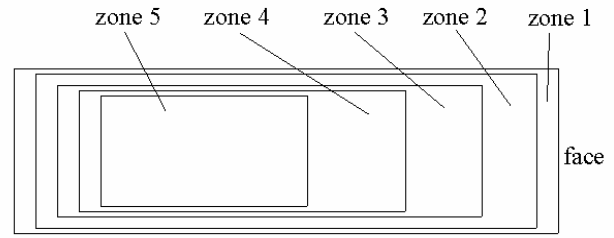

Figure 2. Gob zones for a single longwall panel.

In the gob caved area, the re-compaction of the caved rock has a significant effect on its permeability. Stress changes in the rock in the gob cause changes in the fracture apertures which then impact the permeability. Immediately behind the advancing face, the caved rock is loosely stacked and has a porosity of approximately 0.4. As the mining face advances away from this caved rock, the weight of the overburden gradually increases, which re-compacts the caved rock. This loading or stress in the caved material increases exponentially, until the full overburden load is supported by the caved material. The re-compaction, estimated with the FLAC model's assigned strength and mechanical properties of the gob material, results in a reduction in the void space within the broken rock rubble and, therefore, significant changes in permeability. A simple relationship was used to estimate the changes in permeability in the caved rock based on the Kozeny-Carmen equation:

$$k = f\left(\frac{n^3}{(1-n)^2}\right) \qquad (1)$$

where n is the porosity and k is the permeability.

Using the results of the FLAC model, the permeabilities for the five zones were determined to be 1×10^6 millidarcies (md) for zone 1, 2×10^5 md for zone 2, 7×10^4 md for zone 3, 1×10^4 md for zone 4, and 5×10^3 md for zone 5. The longwall face shields were simulated as a thin porous media with a permeability of 9×10^7 md. Note that the higher permeability in zone 1 provides for lower resistance pathways along the periphery of the gob. It should be pointed out that the permeability data used in this study are different from those used by Brunner (1985), 1×10^{-7} to 1×10^{-5} m^2 (1×10^8 to 1×10^{10} md), Ren et al. (1997), 1×10^{-15} to 1×10^{-10} m^2 (1 to 1×10^5 md), and Wendt et al. (2002), maximum 1×10^{-9} m^2 (1×10^6 md). These differences may be caused by different coal seam geology, different mine panel layout, and different time periods in which the permeability was estimated.

4 NUMERICAL MODELING

A commercial CFD software program, FLUENT™ (Reference to a specific product is for informational purposes and does not imply endorsement by NIOSH), from Fluent, Inc., was used to simulate the air flow in the gob. FLUENT is a general purpose CFD solver for a broad spectrum of flow modeling applications. It has the capability to simulate laminar and turbulent porous media flow based on the known permeability and the inertial resistance factor data. The air flow in the longwall mine gob area is treated as laminar flow in a porous media. The real flow inside a gob can be very complicated, and this laminar flow assumption may not be valid for every region inside a gob. Further research will be carried out that may modify this assumption in the next phase of this program. The air flow in the ventilation airways was simulated as fully developed turbulent flow using standard k-ε equations with k the turbulent kinetic energy, ε the turbulence dissipation rate. The k-ε equations are derived from the eddy viscosity theory of turbulent flow, and have been used successfully to model turbulent flow in many different situations.

The physical model and mesh for the CFD simulation were created using the mesh generation software, GAMBIT, from Fluent, Inc. The cell size varies from 1 to 4 m in the model. They were selected to resolve the flow patterns both in the gob and inside typical mine airways, as well as to achieve an acceptable convergence within a reasonable amount of time. This mesh is depicted in Figure 3. The total cell number for the three-entry bleeder system was 644,660, most of which were hexahedral cells as shown in the figure.
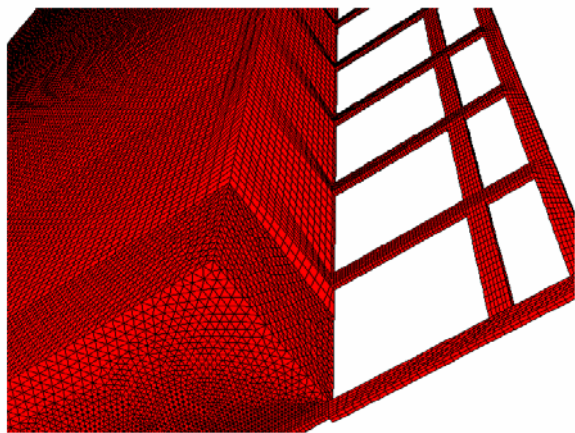

Figure 3. The mesh for the thee-entry bleeder system.

For the simulations with FLUENT, boundary conditions were chosen to represent pressures and flow quantities found in typical longwall ventilation situations for the geometry modeled. For one-entry and the two-entry ventilation systems, the boundary condition used was 0.12 kPa (0.5 inches water gauge) pressure differential between the intake and return entry along the longwall face. To control the air flow quantity to the longwall face, the wall roughness was adjusted to have a realistic intake airflow rate of 30 m^3/s (64,000 cfm).

For the three-entry bleeder ventilation system, two regulators were placed at the end of the second and third intake entry, respectively, as shown in Figure 1 (c), and were simulated as surfaces that can have a pre-defined pressure change. No regulators were placed at the tailgate side of the gob, and the flow was controlled by the permeability value assigned. In actual bleeder ventilation systems, there are usually regulators in the entries at the tailgate side. In the model this simplification was justified since the boundary conditions effectively replace these regulators. The boundary conditions used were -0.62 kPa (-2.5 inches water gauge) pressure at the intake airway inlet on the headgate side of the face, -0.75 kPa (-3 inches water gauge) pressure at the return entry outlet on the tailgate side of the face, and -3.7 kPa (-15 inches water gauge) pressure at the bottom of the bleeder fan shaft. The wall roughness was adjusted to have the total airflow rate of 43 m^3/s (91,000 cfm) for all three intake entries. The pressure drops across the two headgate regulators were also adjusted so that the airflow quantity along the longwall face was the same as longwall face quantities used with the one-entry and two-entry ventilation systems, i.e. 30 m^3/s (64,000 cfm).

5 FLOW PATTERNS INSIDE THE GOB

The air flow inside a gob is expected to be three dimensional with the flow in the vertical direction weaker than in the other two directions. In order to visualize the flow patterns inside the gob, a virtual horizontal reference surface was created 1 m (3 ft) from the bottom of the coal seam floor. All results reported hereafter are with respect to this horizontal reference surface.

5.1 *One-entry bleederless system*

Figure 4 shows the flow path lines for the one-entry bleederless system colored by velocity magnitude. Figure 4 (a) shows the path lines in the entire gob area, and Figure 4 (b) shows the path lines near the face. The path lines show that flow through the gob itself was mainly concentrated behind the shields. At the headgate side, air leaked through the shields but some was forced back into the face again through

the shields near the tailgate side. The air velocity ranged between 1.0×10^{-5} to 1.0×10^{-4} m/s (0.002 to 0.02 fpm) near the shields, and below 1.0×10^{-5} m/s (0.002 fpm) farther away from the shields.
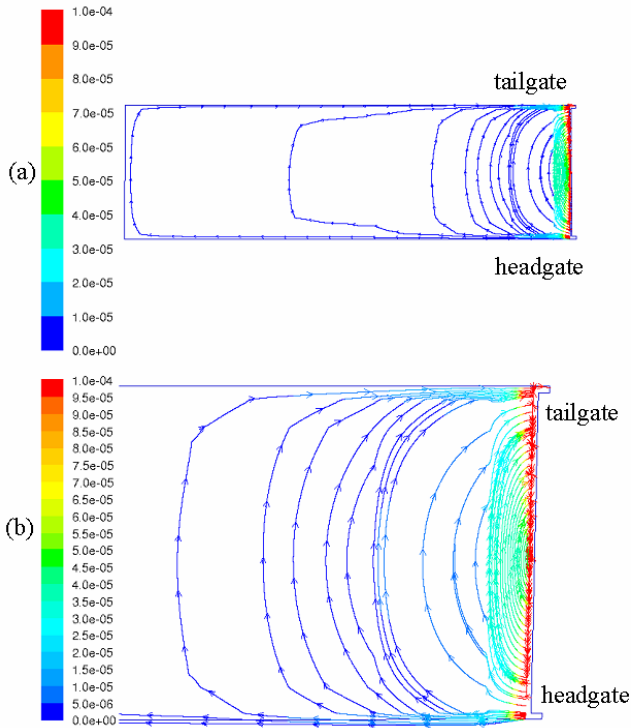

Figure 4. Flow path lines colored by velocity magnitude (m/s) for the one-entry system: (a) in the whole gob; (b) near the shields.

5.2 Two-entry bleederless system

Results of the modeled flow paths for the two-entry bleederless ventilation system were similar to the one-entry system, except for slightly higher air velocities on the tailgate side created by the second return crosscut inby the face shown in Figure 5. For both one-entry and two-entry bleederless ventilation systems, the air flow velocity at the back end of the gob was very low. Figure 6 compares velocity contours close to the shields and near the tailgate between the one-entry and two-entry ventilation systems. The velocity contours were only slightly different between the two systems, indicating that the second return entry has little effect on the velocity field close to the shields. Inside the gob and near the second return entry inside the gob, the air velocity was about 1.0×10^{-4} to 7.0×10^{-4} m/s (0.02 to 0.14 fpm). The air velocity inside the second return entry was about 7.0×10^{-4} to 1.0×10^{-3} m/s (0.14 to 0.2 fpm).
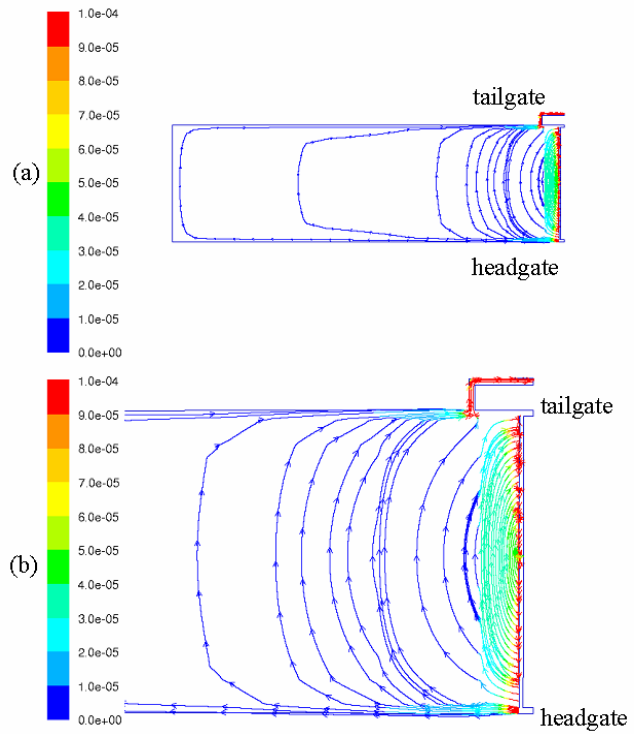

Figure 5. Flow path lines colored by velocity magnitude (m/s) for the two-entry system: (a) in the whole gob; (b) near the shields.
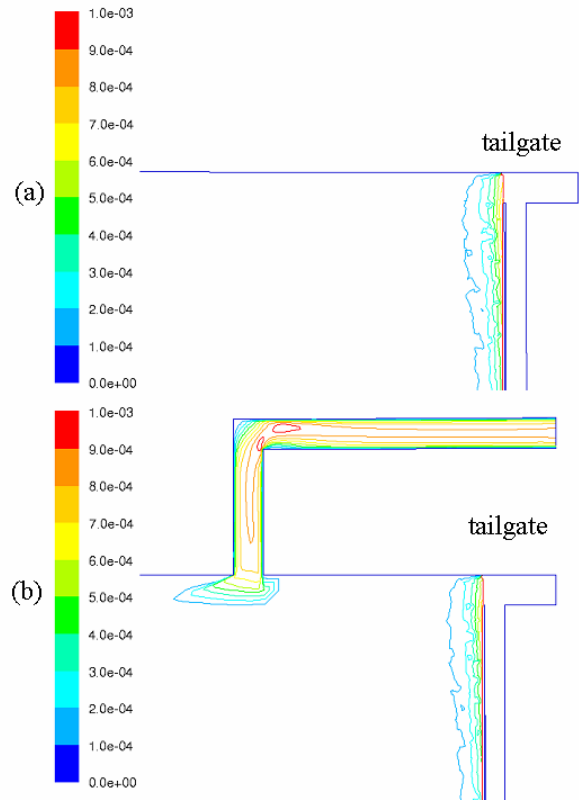

Figure 6. Comparison of colored velocity contours (m/s) between the one-entry and two-entry ventilation system: (a) one-entry system; (b) two-entry system.

5.3 *Three-entry bleeder system*

Figure 7 (a) shows the flow path lines in the gob with the three-entry bleeder ventilation system. A bleeder fan is located at the back of the panel. Gob air flow was mainly concentrated in three areas; behind the shields, near the back end of the gob, and along the tailgate entry, where the permeability is highest compared to other caved zones in the gob. The air velocity along the least compacted zone (zone 1) at the tailgate side was larger than that behind the shields, but smaller than that near the back end of the gob. Figure 7 (b) shows the flow path lines near the shields. Air that leaked through the shields at the headgate side does not flow back into the face at the tailgate side in this ventilation scheme, but flows towards the tailgate side and then out of the gob through the least compacted zone. Some air from the second and third intake entries enters into the gob through the crosscuts near the back end of the gob. The air velocity behind the shields was between 1.0×10^{-3} to 7.0×10^{-3} m/s (0.2 to 1.4 fpm), much higher than was seen for the one-entry and two-entry ventilation systems. Figure 8 (a) shows the flow path lines near the back end of the gob. The air velocity was about 1.0×10^{-2} to 3.0×10^{-2} m/s (2 to 6 fpm), even higher than that behind the shields. Figure 8 (b) shows the flow path lines near the center of the gob. These path lines were directed towards the bleeder fan, but with very low air velocity, about 1.0×10^{-6} to 7.0×10^{-6} m/s (0.0002 to 0.0014 fpm).
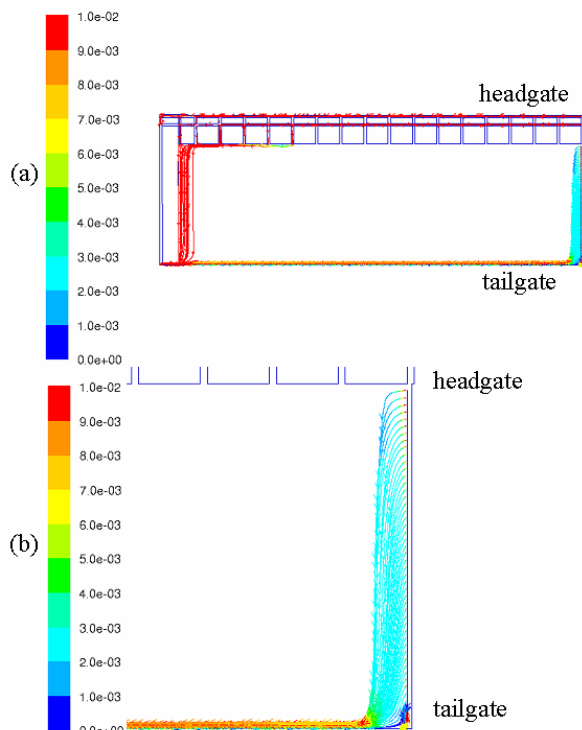

Figure 7. Flow path lines colored by velocity magnitude (m/s) for the three-entry bleeder system: (a) in the whole gob; (b) near the shields.
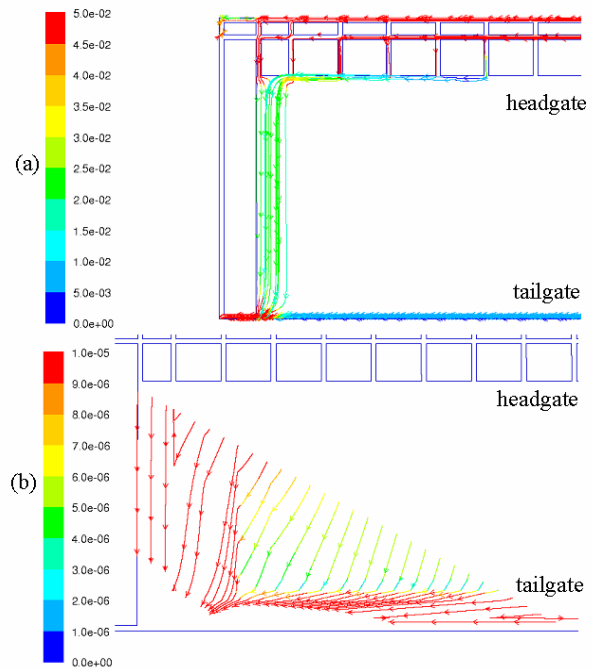

Figure 8. Flow path lines colored by velocity magnitude (m/s) for the three-entry bleeder system: (a) near the back end of the gob; (b) away from the back of the gob.

6 CONDITIONS FOR SPONTANEOUS COMBUSTION

In coalbeds that are reactive to oxidation, critical velocity airflow over reactive coal increases the risk of coal heatings. Critical airflow is defined as insufficient airflow to remove the heat due to oxidation, but sufficient airflow to maintain the oxidation process (Smith et al., 1994). In general, just behind the shields and along the edges of the gob (in the bleeder case), the air velocity is high, so that any heat generated by self-heating is carried away. Deeper in the gob, the air velocity is too low to provide sufficient oxygen to support spontaneous combustion. However, there possibly exists a critical air velocity zone in the gob where the airflow and oxygen concentration are suitable for the continual growth of a self-heating to an eventual fire. The exact range of the critical velocity and its location depend on several factors such as the coal's particle/fragment size, physical and chemical properties, local pressure, temperature, and water vapor concentration. To demonstrate the effect of the ventilation scheme on the critical velocity zone, an estimation for the minimum velocity to carry away heat generated from the self-heating of a 150 µm coal particle was made using the experimental data from Smith & Lazzara (1987).

The self-heating rate of coal under adiabatic condition can be expressed as:

$$dT/dt = A\exp(-E/RT) \qquad (2)$$

where dT/dt is the self-heating rate in K/s, A the pre-exponential factor in K/s, E the activation energy in kcal/mol, and T the temperature in K. Smith & Lazzara (1987) conducted a series of spontaneous combustion studies and determined the activation energy and the pre-exponential factor for a number of U.S. coals. The heat generation rate from the self-heating is:

$$Q = mC_p(dT/dt) \qquad (3)$$

where Q is the heat generation rate in W, m the mass of the particle in g, C_p the specific heat of coal in J/(g·K) at constant pressure. In order to prevent the occurrence of self-heating, the generated heat needs to be carried away by the airflow. The convective heat transfer rate can be expressed as:

$$Q = Sh\Delta T \qquad (4)$$

where S is the particle surface area for convective heat transfer in m^2, h the heat transfer coefficient in W/(m^2·K),)T the temperature differential between the particle and the airflow in K. The heat transfer coefficient h is related to a non-dimensional Nusselt number Nu as:

$$Nu = hl/\lambda \qquad (5)$$

where l is the diameter of the particle in m, λ the heat conductivity of air in W/(m·K). For the laminar flow over a sphere, the Nu number correlates with the Re number as (Kays, 1966):

$$Nu = 0.292\,Re^{1/2} \qquad (6)$$

here $Re = ul/\upsilon$ with u the airflow velocity in m/s, υ the kinematic viscosity of air in m^2/s.

Using an example of the Wyoming No. 80 seam coal particle with l = 0.15 mm, the maximum particle diameter used by Smith & Lazzara (1987), A = 6.9×10^6 K/s, E = 16.8 kcal/mol, T = 60ºC (333 K) and)T = 40 K for the No. 80 seam coal particle, coal specific heat C_p = 1.17 J/(g·K), air heat conductivity λ = 2.59×10^{-4} J/(cm·s·K), and ν = 15×10^{-6} m^2/s, the upper bound for the critical airflow velocity calculated using equations (2) to (6) was 1.1×10^{-4} m/s (0.02 fpm). The minimum airflow velocity (lower bound for critical velocity) required to provide sufficient oxygen to sustain the self-heating will be determined by incorporating the model of kinetic reaction of coal self-heating into the CFD modeling in the next stage of this program.

Figure 9 shows the velocity contour of 1.1×10^{-4} m/s for the three ventilation systems. The critical velocity zone for the particle size of 150 μm should start from this contour towards the lower velocity area. Thus, in this example for the No. 80 seam coal using a one-entry and two-entry bleederless ventilation system, the critical velocity zone started immediately behind the shields towards the center of the gob. Closer to the headgate and the tailgate, the zone started a short distance behind the shields. For the three-entry ventilation system, the critical velocity zone was pushed away both from the shields and from the back end of the gob towards the center. Under these simulation conditions, the velocity contour line was close to the boundary between zone 1 and zone 2 as shown in Figure 2.
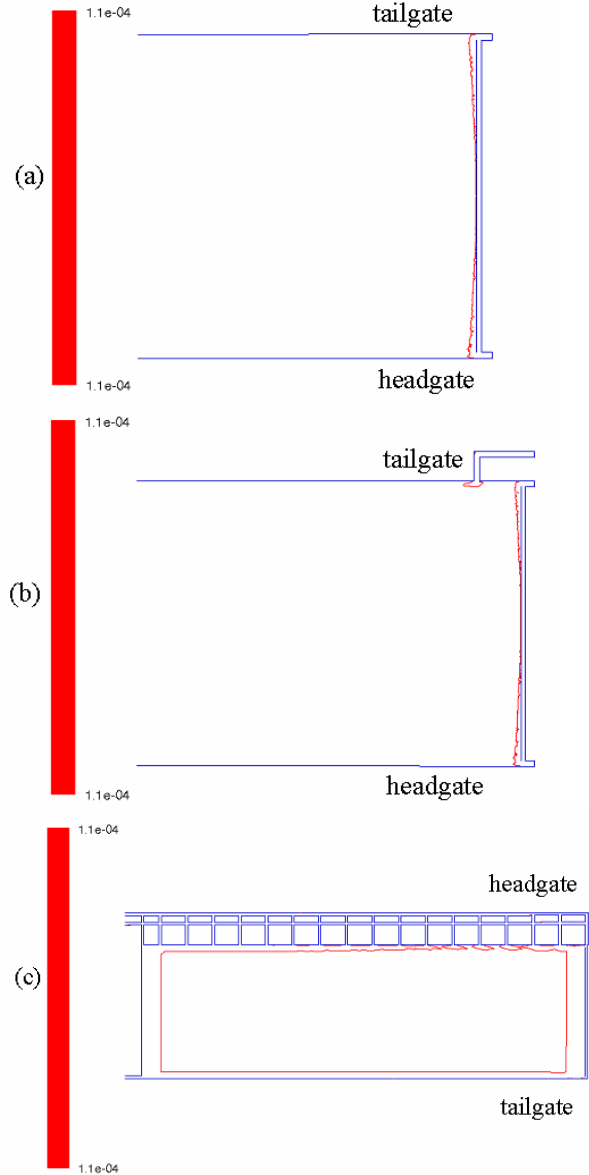

Figure 9. Velocity contour of 1.1×10^{-4} m/s for the three ventilation systems: (a) one-entry bleederless system; (b) two-entry bleederless system; (c) three-entry bleeder system.

7 CONCLUSIONS

CFD simulations were conducted to investigate the air pathways in the gob area under different ventilation schemes. The air flow patterns in the gob were

visualized by flow path lines, velocity contours and velocity vectors. For the one-entry and two-entry bleederless ventilation systems, the flow patterns in the gob were very similar. Only a slightly higher velocity zone occurred near the second return entry with the two-entry ventilation system. This demonstrates that sudden changes in airflow resistance can potentially constitute zones with critical velocities that support spontaneous combustion.

The air velocity was about 1.0×10^{-5} to 1.0×10^{-4} m/s (0.002 to 0.02 fpm) near the shields, and 1.0×10^{-4} to 7.0×10^{-4} m/s (0.02 to 0.14 fpm) near the second intake entry. The velocity near the back end of the gob was very low. For the three-entry bleeder system, the air velocity was much higher behind the shields than with the bleederless systems, about 1.0×10^{-3} to 7.0×10^{-3} m/s (0.2 to 1.4 fpm). There was also high velocity air flow near the back end of the gob, about 1.0×10^{-2} to 3.0×10^{-2} m/s (2 to 6 fpm).

A preliminary calculation for a coal particle size of 150 µm in diameter and similar reactivity to the coal used in this study shows the potential critical velocity zones may occur immediately behind the shields towards the center of the gob for the one-entry and two-entry ventilation systems. For the three-entry bleeder ventilation system, the critical velocity zone may occur farther away from both the shields and the back end of the gob where a permeability gradient exists.

A gob will have coal particles of variable sizes. For any single particle size, there are multiple solutions for particle temperature T and temperature difference between particle and air. Therefore, it is difficult to develop a unique solution. However, the goal is to outline areas with spontaneous combustion potential. Future work will be done to further investigate the flow patterns and to simulate the effect of methane control measures on the air flow patterns inside the gob in mines with appreciable methane levels. It is also intended to verify the results of the CFD model by using tracer gas and quantity/pressure surveys where possible.

ACKNOWLEDGMENTS

REFERENCES

Balusu, R., Deguchi, G., Holland, R., Moreby, R., Xue, S., Wendt, M. & Mallett, C. 2002. Goaf gas flow mechanics and development of gas and Sponcom control strategies at a highly gassy mine. *Coal and Safety* 20: 35-45.

Banik, J., McPherson, M.J. & Topuz, E. 1995. Ventilation control of self-heating in retreating longwall coal mines. *Proceedings of the 7th US Mine Ventilation Symposium*, *Lexington, 5-7 June*.

Brune, J.F., Aman, J.P. & Kotch, M. 1999. Developments in Longwall Ventilation. *Proceedings of the 8th US Mine Ventilation Symposium*, *Rolla, 14-17 June*.

Brunner, D.J. 1985. Ventilation models for longwall gob leakage simulation. *Proceedings of the 2nd US Mine Ventilation Symposium*, *Reno, 23-25 September*.

DeRosa, M. 2004. Analysis of mine fires for all U.S. underground and surface coal mining categories, 1990-1999. *NIOSH Information Circular 9470*.

Esterhuizen, G. S. & Karacan, C.O. 2005. Development of Numerical Models to Investigate Permeability Changes and Gas Emission Around Longwall Mining Panels. *Proc. AlaskaRocks 2005, 40th US Symposium on Rock Mechanics, Anchorage, 25-26 June*.

Kays, W.M. 1966. *Convective Heat and Mass Transfer*. McGraw-Hill.

Ren, T.X., Edwards, J.S. & Jozefowicz, R.R. 1997. CFD modeling of methane flow around longwall coal faces. *Proceedings of the 6th International Mine Ventilation Congress, Pittsburgh, 17-22 May*.

Smith, A.C., Diamond, W.P., Mucho, T.P. & Organiscak, J.A. 1994. Bleederless Ventilation Systems as a Spontaneous Combustion Control Measure in U.S. Coal Mines. *US Bureau of Mines Information Circular 9377*.

Smith, A.C. & Lazzara, C.P. 1987. Spontaneous Combustion Studies of U.S. Coals. *US Bureau of Mines Report of Investigations 9079*.

Wala, A., Jacob, J., Brown, J. & Huang, G. 2003. New approaches to mine-face ventilation. *Mining Engineering*, March, 25-30.

Wendt, M. & Balusu, R. 2002. CFD modeling of longwall goaf gas flow dynamics. *Coal and Safety* 20: 17-34.